1   **Supplemental Data**

2   **Figure 1.**

3
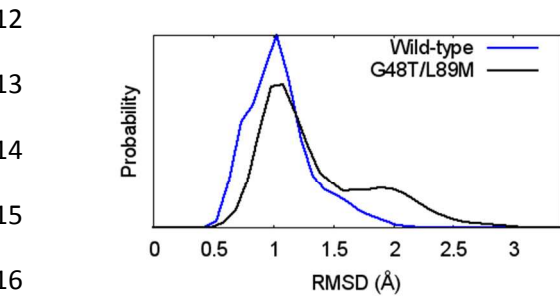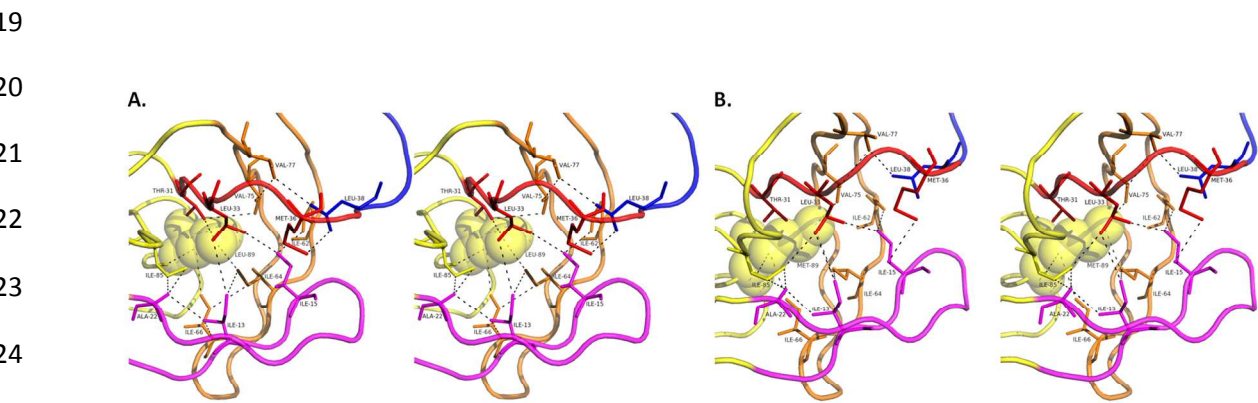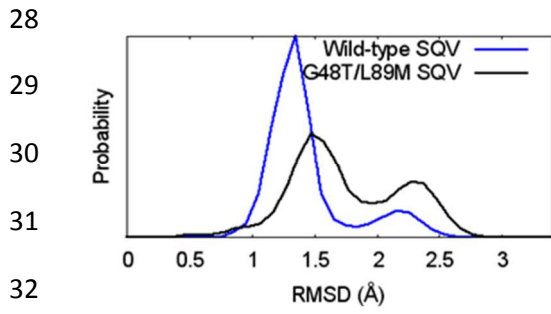

11   **Figure 2.**

17

18   **Figure 3.**

19

27   **Figure 4.**

28

29

30

31

32
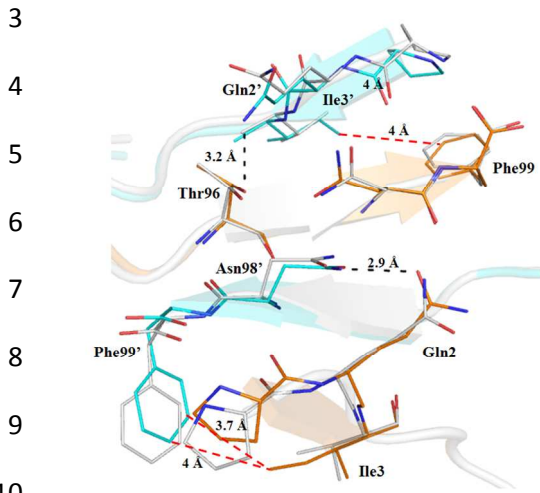
33

34

35   **Figure 5.**

36

37

38

39

40

41

42

43
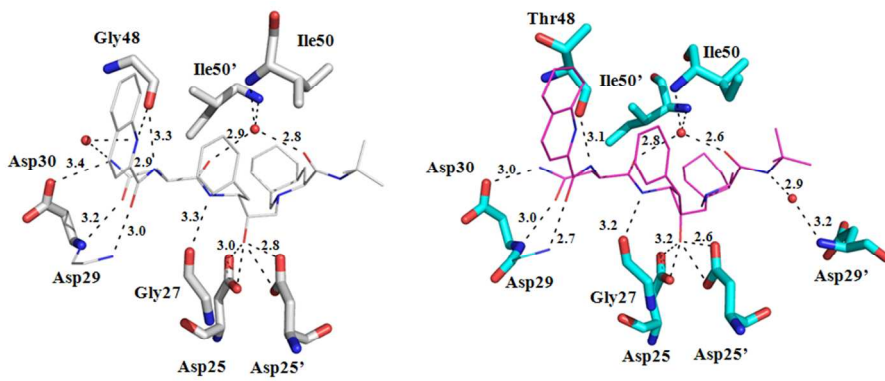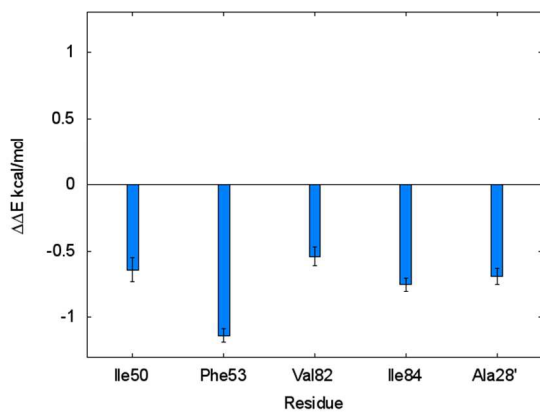
44

45   **Figure 6.**

46

47

48

49

50

51

52

Supplementary Figure Legends

Figure 1. PR_{WT-SQV} is shown in silver and $PR_{G48T/L89M-SQV}$ is shown in orange (monomer A) and cyan

(monomer B). A 180° rotation of the side chain of Gln2 and a 180° rotation of the side chain of Asn98' in

$PR_{G48T/L89M-SQV}$ results in a new hydrogen bond (2.9 Å) between the O_ε of Gln2 and the δN-H of Asn98'.

A new hydrogen bond (3.2 Å) is also formed between the O_ε of Gln2' and the O_γ-H of Thr96. Two

interdomain vdw contacts are gained between Ile3 and Phe99', as well as one new vdw contact between

Ile3' and Phe99. These new interactions in the terminal domain contribute to a more stable dimer relative

to PR_{WT-SQV}.

Figure 2. A histogram of the root mean squared deviation of the flaps' Cα atoms (residues 43-58 of each

monomer) obtained through the molecular dynamics simulations. $PR_{G48T/L89M-SQV}$ exhibits a decrease in

peak intensity at 1 Å and an appearance of a peak at 2 Å compared to PR_{WT-SQV}. These results suggest that

the flaps of $PR_{G48T/L89M-SQV}$ are more open relative to $PR_{WT-SQV.}$

Figure 3. Stereo images of hydrophobic core residues in monomer A of **A)** PR_{WT-SQV} and **B)** $PR_{G48T/L89M-}$

$_{SQV}$. PR is color coded to represent the fulcrum (magenta: 11-22), cantilever (orange: 58-78), elbow flap

(blue: 39-57), and 30's strand (red). Vdw interactions are shown as black dashed lines. In PR_{WT-SQV}, vdw

interactions are amenable for hydrophobic sliding; however, in $PR_{G48T/L89M-SQV}$ a redistribution of vdw

forces results in altered strand interactions and modified hydrophobic sliding.

Figure 4. A histogram of the root mean squared deviation of saquinavir. It compares the mobility of

saquinavir in the active site of PR_{WT} and $PR_{G48T/L89M}$ during the molecular dynamics simulations. The

RMSD profile of saquinavir in $PR_{G48T/L89M}$ exhibits a marked decrease in peak intensity at ~1.3 Å and

new peaks at higher RMSD values of 1.5 and ~2.3 Å compared to that of PR_{WT} indicating that saquinavir

is more mobile in the active site of $PR_{G48T-L89M-SQV}$.

77   **Figure 5.** PR_{WT-SQV} is shown in silver and $PR_{G48T/L89M-SQV}$ is shown in cyan and magenta. Hydrogen bonds

78   are shown as dashed lines and distances are noted in Angstroms. The conserved water linking the PR

79   flaps and saquinavir are present between the amide nitrogens of Ile50/50' and O1 and O3 of SQV in both

80   structures. However, in the $PR_{G48T/L89M-SQV}$ complex the hydrogen bond from the carbonyl of Thre48 to N1

81   of the quinolone ring is missing.

82   **Figure 6.** A plot of a per-residue decomposition of the van der Waals energetics that only includes

83   residues that interact with saquinavir. The differences between PR_{WT-SQV} and $PR_{G48T-L89M-SQV}$ are shown

84   where a negative number indicates that the van der Waals interaction with saquinavir is more favorable in

85   PR_{WT-SQV}. Only residues with differences greater than 0.5 kcal/mol were plotted.

86

87

88